Supplementary Material (ESI) for Dalton Transactions
This journal is © The Royal Society of Chemistry 2013

Electronic Supplementary Information (ESI) for Dalton Transactions

Neutral Copper(I) Dipyrrin Complexes and their use as Dye Sensitizers in Dye-Sensitized Solar Cells

Tracy E. Hewat, Lesley J. Yellowlees, and Neil Robertson *

School of Chemistry and EaStChem, University of Edinburgh,

King's Buildings, Edinburgh, UK.

Fax: +44 131 650 4743; Tel: +44 131 650 4755;

E-mail: neil.robertson@ed.ac.uk

Experimental

Synthesis of 4,4'-(CO_2Et)-6,6'-dimethyl-2,2'-bipyridine (dmdecbpy)

Dmdcbpy (400 mg, 1.47 mmol) and conc. sulfuric acid (7.8 mL) were added to ethanol (86 mL) and refluxed under nitrogen for 72 h. The solution was cooled down, poured over crushed ice and was kept in the fridge overnight. The solvent was reduced to half the volume under reduced pressure. 1M NaOH was added until a precipitate formed, ensuring the solution was kept at pH 1. The white solid was filtered off and washed with water. Yield: 56 %, 273 mg. ^{1}H NMR (DMSO, 400 MHz): δ 8.61 (s, 2H, H-bpy), 7.79 (s, 2H, H-bpy), 4.41 (q, 4H, O-**CH_2,** J_{HH} = 7.2 Hz), 2.67 (s, 6H, CH_3), 1.36 (t, 6H, CH_2**CH_3**, J_{HH} = 7.1 Hz). +ESI/MS: *m/z* 329.2 (M^+). Anal. Calc. for $C_{18}H_{20}N_2O_4$: C 65.84, H 6.14, N 8.53. Found: C 65.71, H 6.10, N 8.68.

Step 1 of HL3 synthesis (4-(Ethoxy)-1,1,1-trifluoro-3-butene-2-one)

4-dimethylaminopyridine (12 mg, 0.1 mmol), and trifluoroacetic anhydride (328 mg, 15.62 mmol) were added to DCM (20 mL) and cooled to -10 ^{o}C. Ethyl vinyl ether (106 mg, 14.7 mmol) was added dropwise to the solution. The reaction mixture was stirred at 0 ^{o}C for 19 h. The solution was warmed to room temperature and the solvent was removed under reduced pressure. The purple oil was poured into sodium bicarbonate solution to produce a yellow oil. The phases were extracted and separated and the organic layer was dried over anhydrous Na_2SO_4. The solvent was removed under reduced pressure to yield a red/orange oil. Yield: 267 mg, 10.8 %. ^{1}H NMR ($CDCl_3$, 400 MHz): δ 7.89 (d, 1H, J = 12.1 Hz, CH), 5.85 (d, 1H, J = 12.2 Hz, CH), 4.10 (q, 2H, J = 7, 14.3 Hz, CH_2), 1.40 (t, 3H, J = 6.9, 14.3 Hz, CH_3).

Step 2 of HL3 synthesis (1-[2-hydroxy-4-(trifluoromethyl)phenyl]ethanone)

NaH (240 mg, 10 mmol) was placed under argon and cooled down to 0 ^{o}C. Dry THF (10 mL) was added to NaH via cannula. 4-(Ethoxy)-1,1,1-trifluoro-3-butene-2-one (840 mg, 5 mmol) and acetylacetone (500 mg, 5 mmol) were transferred to the reaction mixture slowly. The mixture was warmed to room temperature and then refluxed for 3 h. The solution turned from yellow to red. The mixture was cooled to room temperature. 1M HCl was added until the solution reached pH 3. The mixture was separated and extracted with DCM (3x40 mL) and the organic layer was dried over $MgSO_4$. The solvent was removed under reduced pressure to yield a yellow/brown oil. The sample was purified on silica (hexane/ethyl acetate 90:10) to yield a yellow oil. Yield: 195 mg, 10.5 %. ^{1}H NMR ($CDCl_3$, 400 MHz): δ 12.28 (s, 1H, OH), 7.86 (d, 1H, J = 8.3 Hz, ar), 7.25 (d, 1H, J = 1.8 Hz, ar), 7.15 (dd, 1H, J = 1.8, 8.2 Hz, ar), 2.68 (s, 3H, CH_3).

Step 3 of HL3 synthesis

Benzhydrazide (130 mg, 9.5 mmol) and 1-[2-hydroxy-4-(trifluoromethyl)phenyl]ethanone (195 mg, 9.5 mmol) were added to *n*-propanol and refluxed overnight. The reaction mixture was cooled to room temperature and filtered. The crude product was recrystallised from boiling *n*-propanol to yield a white crystalline product. Yield: 159 mg, 51.7 %. ^{1}H NMR (DMSO, 500 MHz): δ 13.77 (s, 1H, NH), 11.50 (s, 1H, OH), 7.95 (d, 2H, J = 7.6 Hz, Ph), 7.86 (d, 1H, J = 7.6 Hz, ar), 7.64 (t, 1H, J = 7.6 Hz, Ph), 7.56 (t, 2H, J = 7.6 Hz, Ph), 7.22 (d, 1H, J = 7.6 Hz, ar), 7.22 (s, 1H, ar), 2.53 (s, 3H, CH_3). ^{13}C NMR (DMSO, 128.1 MHz): δ 164.7, 158.8, 156.4, 132.7, 132.1, 129.7, 128.4, 128.2, 122.9, 122.7, 114.6, 113.9, 14.2. +ESI/MS: 323.11 [M+H]. $C_{16}H_{13}F_3N_2O_2$: C 59.63 H 4.07 N 8.69. Found C 59.76 H 3.85 N 8.78.

Step 4 of HL3 synthesis

The product from step 3 was added to THF at 25 ^{o}C. Lead(IV) acetate was added slowly to the solution. The reaction mixture was stirred for 1 h then filtered. The filtrate was separated and extracted with DCM, water, and then brine. The organic extracts were dried over $MgSO_4$. The solvent was removed under reduced pressure. The crude product was purified on alumina Act(IV) (DCM/cyclohexane 40:60) to yield a white solid. Yield: 859 mg, 86.4 %. ^{1}H NMR ($CDCl_3$, 500 MHz): δ 7.97 (d, 1H, J = 8.3 Hz, ar), 7.86 (dd, 1H, J = 8.3 Hz, ar), 7.74 (dd, 2H, J = 7.8 Hz, Ph), 7.67 (s, 1H, ar), 7.59 (tt, 1H, J = 7.8 Hz, Ph), 7.46 (t, 2H, J = Hz, 7.8 Ph), 2.56 (s, 3H, CH_3). ^{19}F NMR (DMSO, 376 MHz): δ -63.10. +ESI/MS: 293.08 [M+H]. $C_{16}H_{11}F_3O_2$: C 65.76 H 3.79 N 0. Found C 65.83 H 3.84 N 0.

Step 5 of HL3 synthesis

The product from step 4 was added to acetic acid (12.4 mL) and methanol (24.6 mL). Ammonium hydroxide (conc. 6.2 mL) was added dropwise to the solution. The mixture was stirred at room temperature for 24 h. The mixture was filtered and the solid was dissolved in chloroform, and separated and extracted with water (2x30 mL). The organic extracts were dried over $MgSO_4$ and the solvent was removed under reduced pressure. The crude product was purified on silica ($CHCl_3$) to yield a purple solid. Yield: 210 mg, 29.4 %. ^{1}H NMR (DMSO, 500 MHz): δ 13.86 (s), 12.53 (s), 11.52 (s), 8.60 (d), 8.57 (d), 8.31 (s), 8.16 (d), 8.15 (d), 8.09 (d), 8.07 (s), 7.98 (d), 7.94 (d), 7.83 (s), 7.77 (s), 7.69 (d), 7.67 (t), 7.58 (t), 7.52 (t), 7.50 (s), 7.45 (t), 7.34 (d), 7.29 (t), 6.73 (dd). ^{19}F NMR (DMSO, 376 MHz): δ -60.07 (2), -60.17 (2), -60.19 (1), -60.26 (1), -60.28 (1), -60.40 (2). +ESI/MS: 532.41 [M^+]. $C_{31}H_{18}F_6N_2$: C 69.92 H 3.41 N 5.26. Found C 70.05 H 3.51 N 5.36.

Reaction Scheme of HL3 ligand

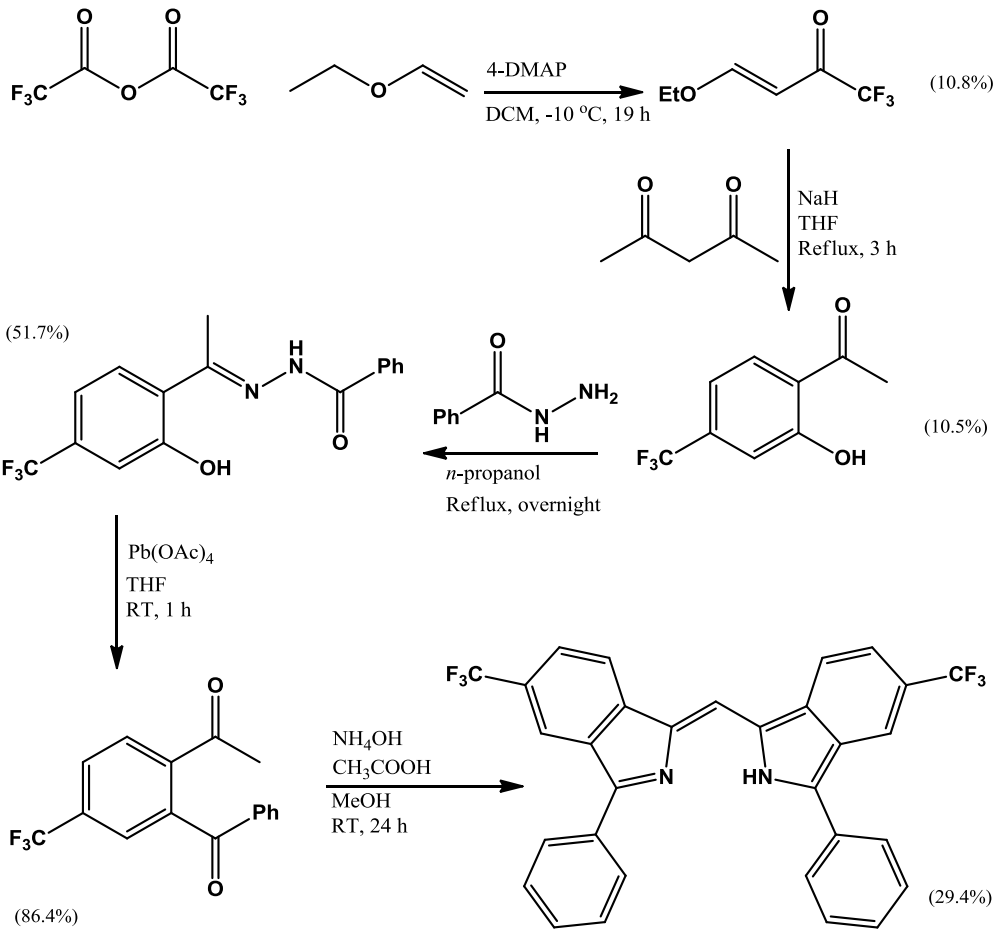

Figure S1 Reaction scheme for the synthesis of HL3.

Stability Tests

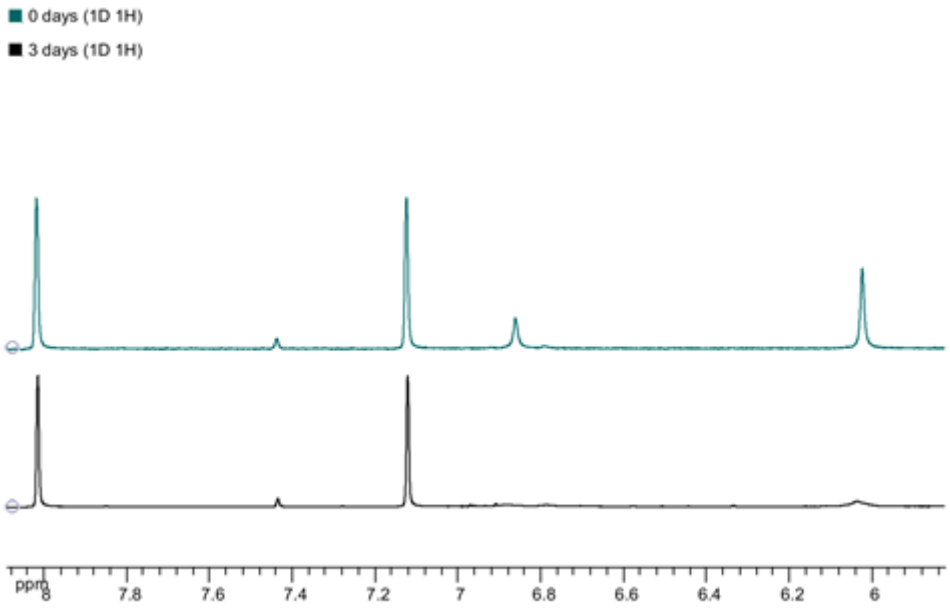

Figure S2 Stability tests of complex **1** in d_6-DMSO. The blue curve represents the initial ^{1}H NMR and the black curve is the NMR after 3 days in solution.

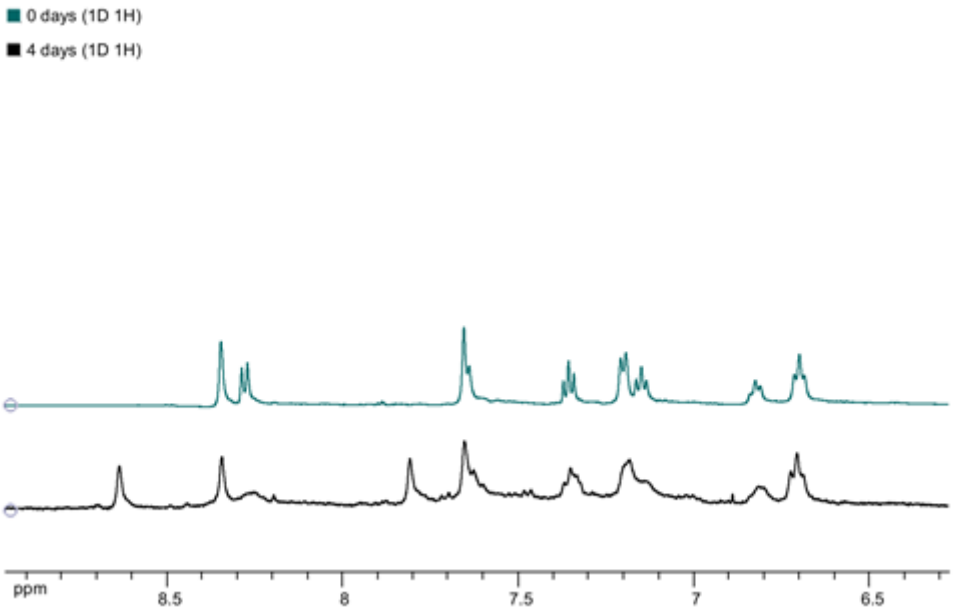

Figure S3 Stability tests of **3** in d_6-DMSO via ^{1}H NMR.

Supplementary Material (ESI) for Dalton Transactions
This journal is © The Royal Society of Chemistry 2013

NMR Studies

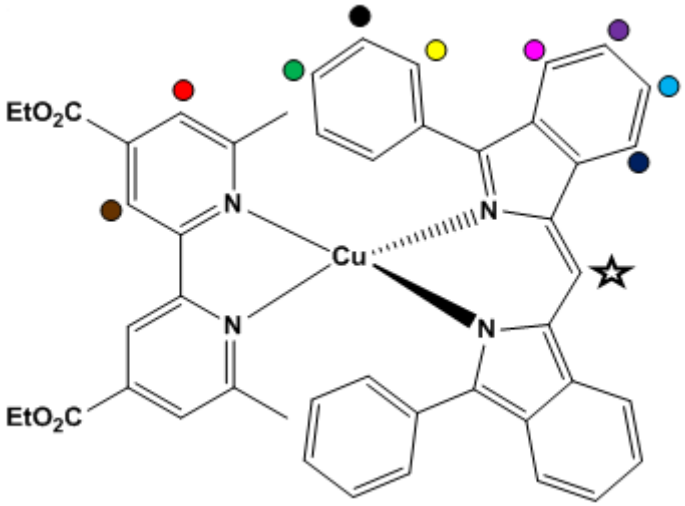

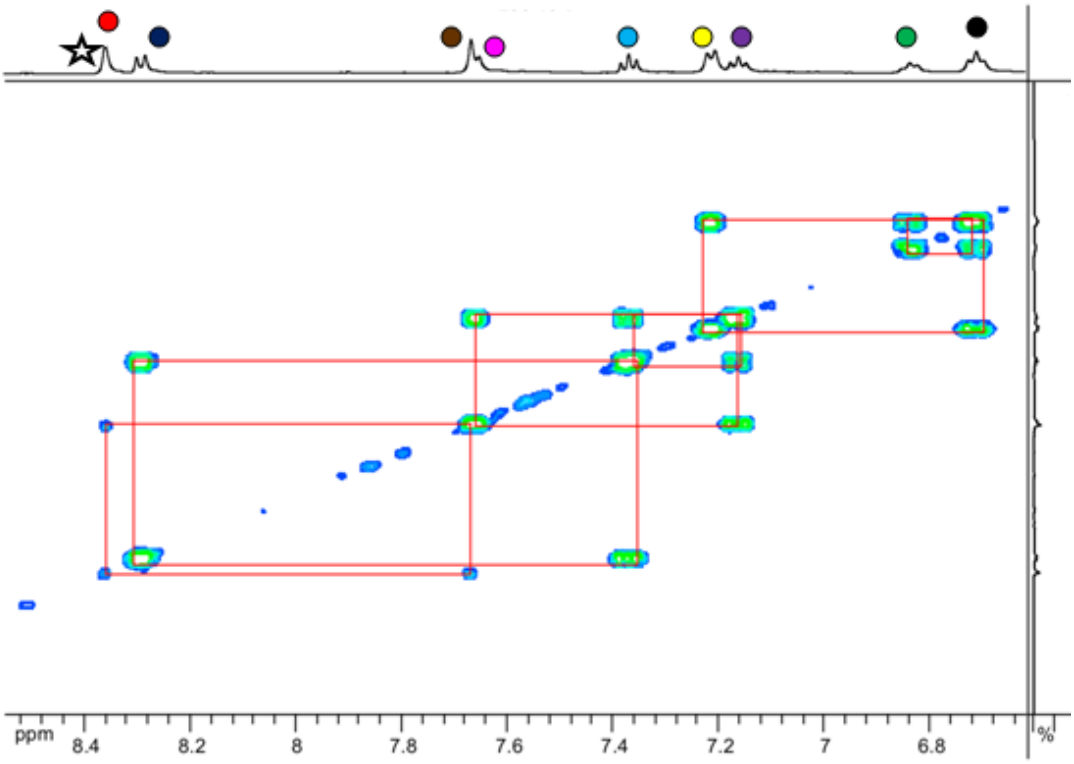

Supplementary Material (ESI) for Dalton Transactions
This journal is © The Royal Society of Chemistry 2013

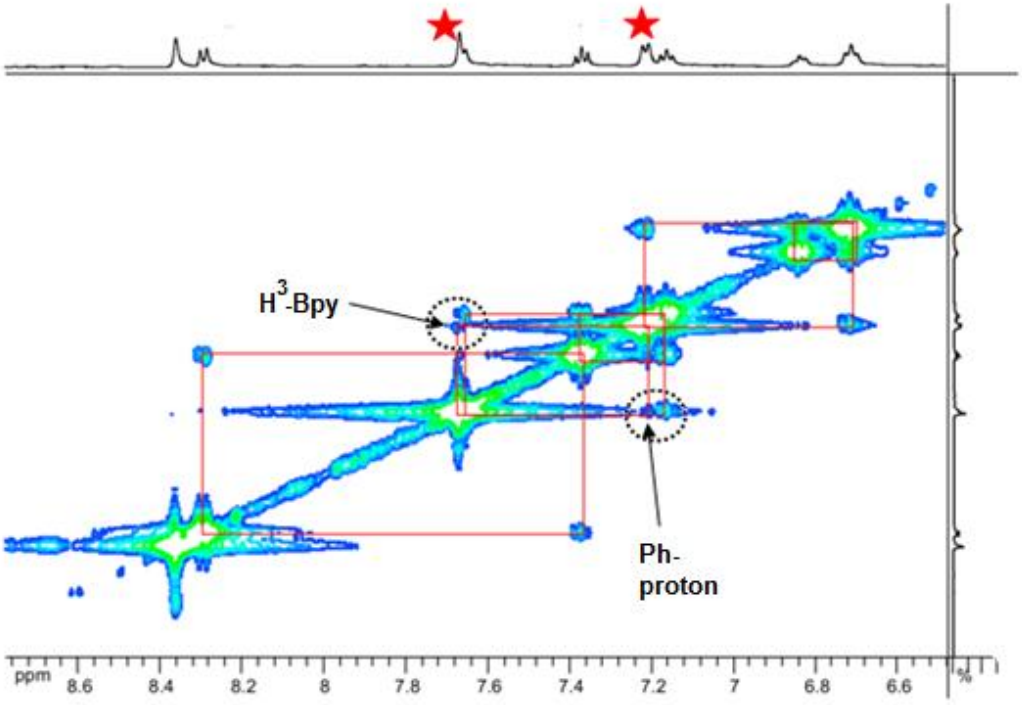

Figure S4 2D COSY (top spectrum) and 2D NOESY (bottom spectrum) of **3**. Each peak can be assigned to the protons featured in the structure of the molecule. It is shown that the Ph-proton from the dipyrrin ligand correlates through space with H^3-bpy, suggesting a tetrahedral geometry.

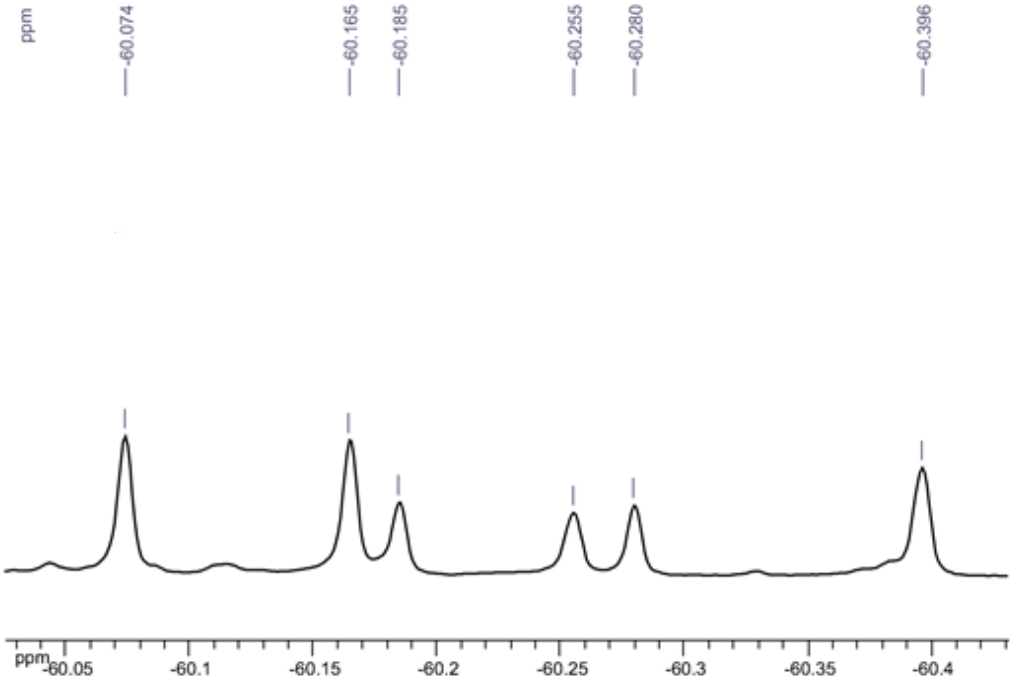

Figure S5 ^{19}F NMR of HL3. Multiple peaks suggest presence of geometrical isomers.

Supplementary Material (ESI) for Dalton Transactions
This journal is © The Royal Society of Chemistry 2013

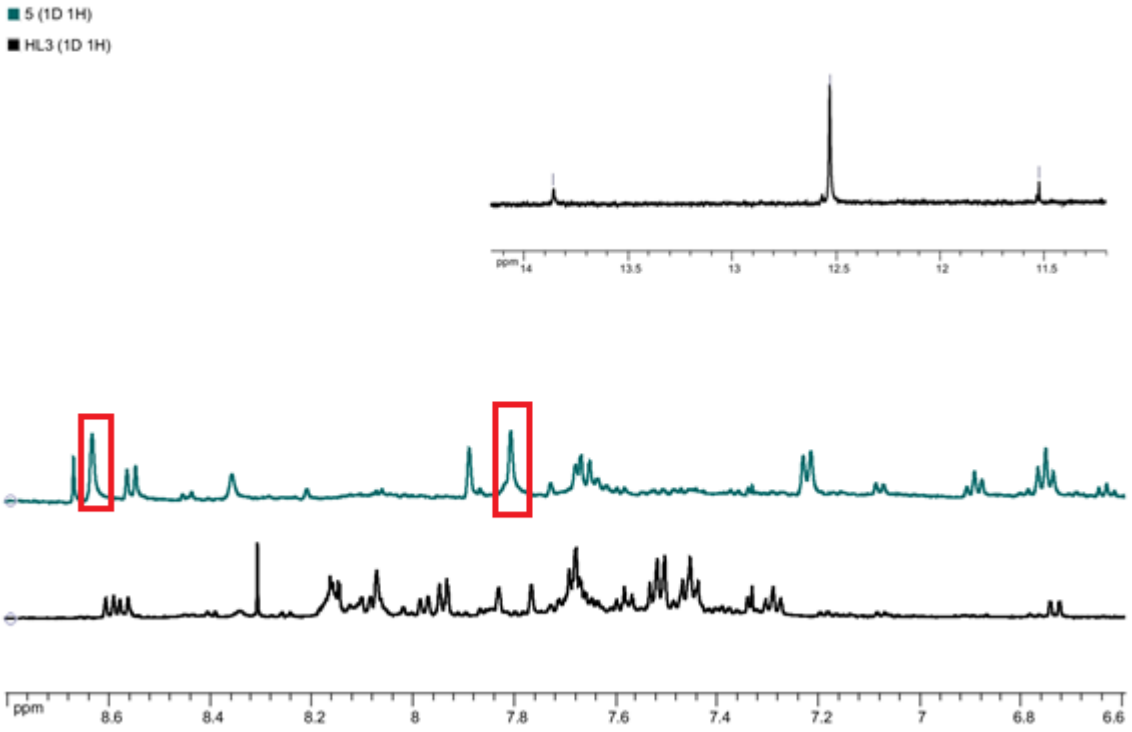

Figure S6 ^{1}H NMR of **HL3** (black line) and **5** (green line). The top spectrum shows the three NH peaks (1:5:1) from **HL3** representing the three isomers. The red box shows the presence of free dmdecbpy ligand.

Absorption Spectroscopy

(a)

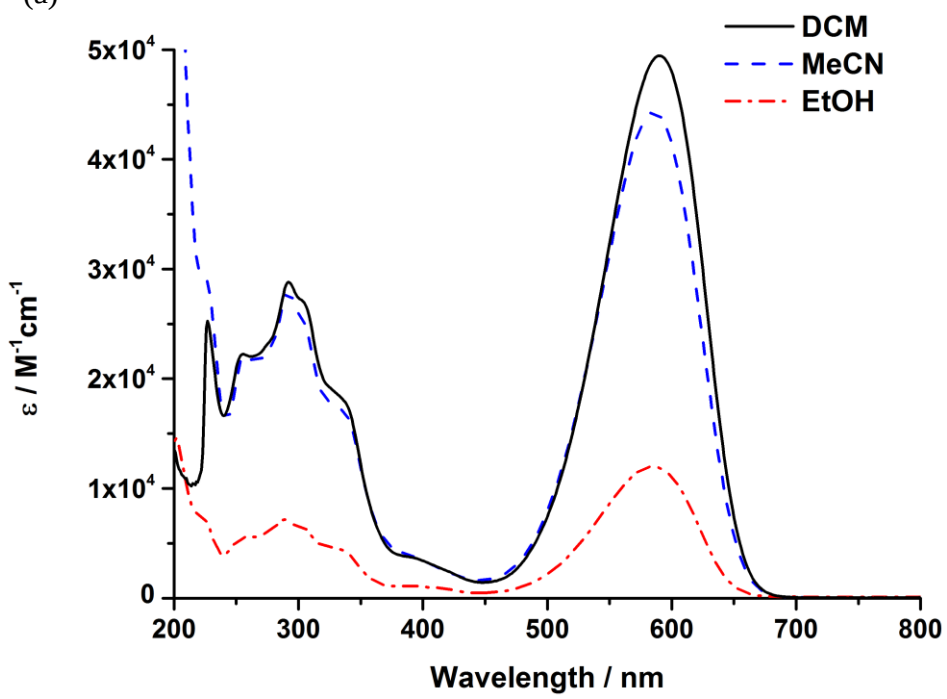

Supplementary Material (ESI) for Dalton Transactions
This journal is © The Royal Society of Chemistry 2013

(b)

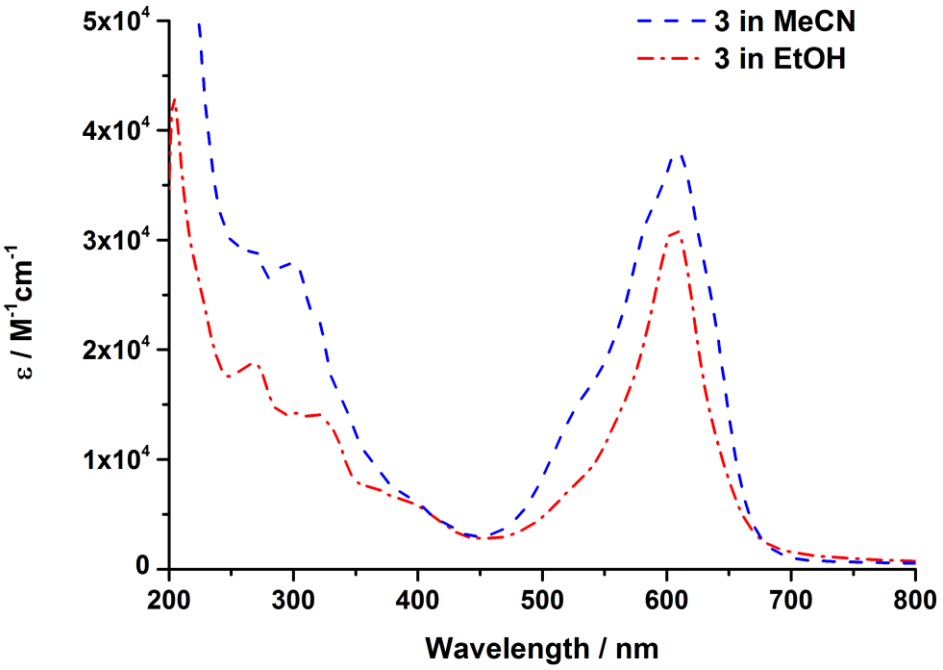

Figure S7 (a) Absorption spectrum of **HL2** in varying solvents (dichloromethane, acetonitrile, and ethanol, and (b) Absorption spectrum of **3** in acetonitrile and ethanol.

Emission Spectroscopy

(a)

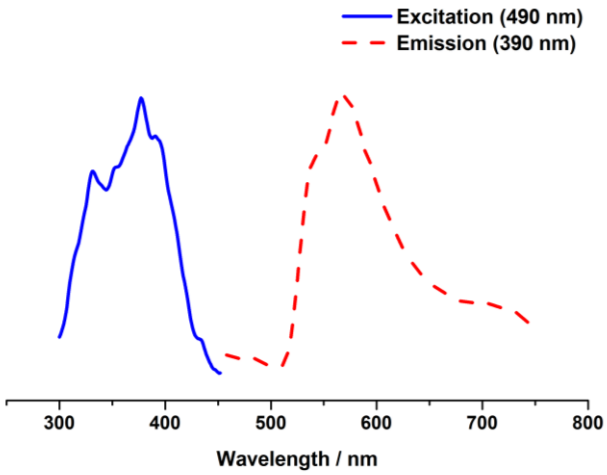

Supplementary Material (ESI) for Dalton Transactions
This journal is © The Royal Society of Chemistry 2013

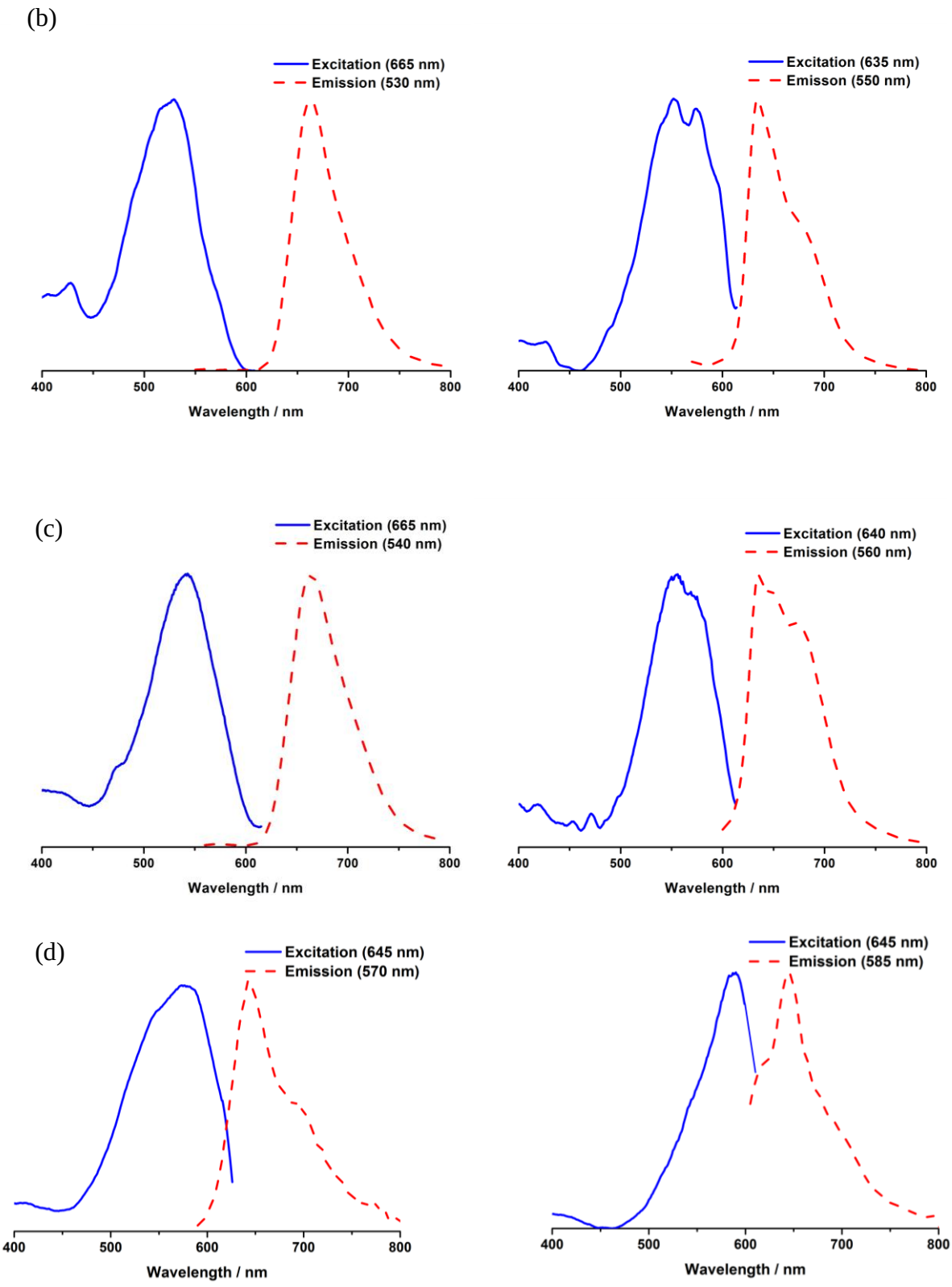

Figure S8 Represents the excitation and emission spectra at room temperature (left) and 77 K (right) for (a) **1**, (b) **2**, and (c) **3**, all were carried out in ethanol and (d) **4** was carried out in acetonitrile.

Computational

Complex	MO	MO energy / eV	% Contribution from		
			Cu-based orbitals	Dipyrrin-based orbitals	Me-Bpy based orbitals
1	HOMO-10	-7.74	2.74	0.54	96.72
	HOMO-9	-7.30	0.27	99.19	0.54
	HOMO-8	-6.75	2.18	2.18	95.64
	HOMO-4	-5.46	68.14	29.68	2.18
	HOMO-3	-5.40	81.52	9.62	8.86
	HOMO-2	-4.95	0.14	99.86	0
	HOMO-1	-4.80	66.58	13.32	20.1
	HOMO	-4.72	68.18	20.82	11
	LUMO	-1.94	3.26	2.19	94.55
	LUMO+1	-1.79	1.49	97.52	0.99
	LUMO+2	-1.01	1.76	1.36	96.88
	LUMO+3	-0.73	0.49	0.32	99.19
	LUMO+4	-0.28	0.04	0.12	99.84
	LUMO+8	-1.52	0.54	98.89	0.57

Table S1 Percentage contributions from component parts of **1** to selected molecular orbitals, and the calculated energies for these molecular orbitals.

Complex	Main Visible Absorbance / nm	Main Charge Transitions MO from	MO to	Relative Contribution
1	581	HOMO-1	LUMO	23 %
		HOMO-1	LUMO+1	36 %
		HOMO	LUMO	41 %
	399	HOMO-4	LUMO+1	12 %
		HOMO-2	LUMO+1	88 %
	287	HOMO-10	LUMO	10 %
		HOMO-8	LUMO	64 %
		HOMO-8	LUMO+2	11 %
		HOMO-1	LUMO+4	15 %
	237	HOMO-9	LUMO+2	75 %
		HOMO-2	LUMO+8	25 %

Table S2 Percentage contributions from component parts of **1** to selected molecular orbitals, and the calculated energies for these molecular orbitals.

Supplementary Material (ESI) for Dalton Transactions
This journal is © The Royal Society of Chemistry 2013

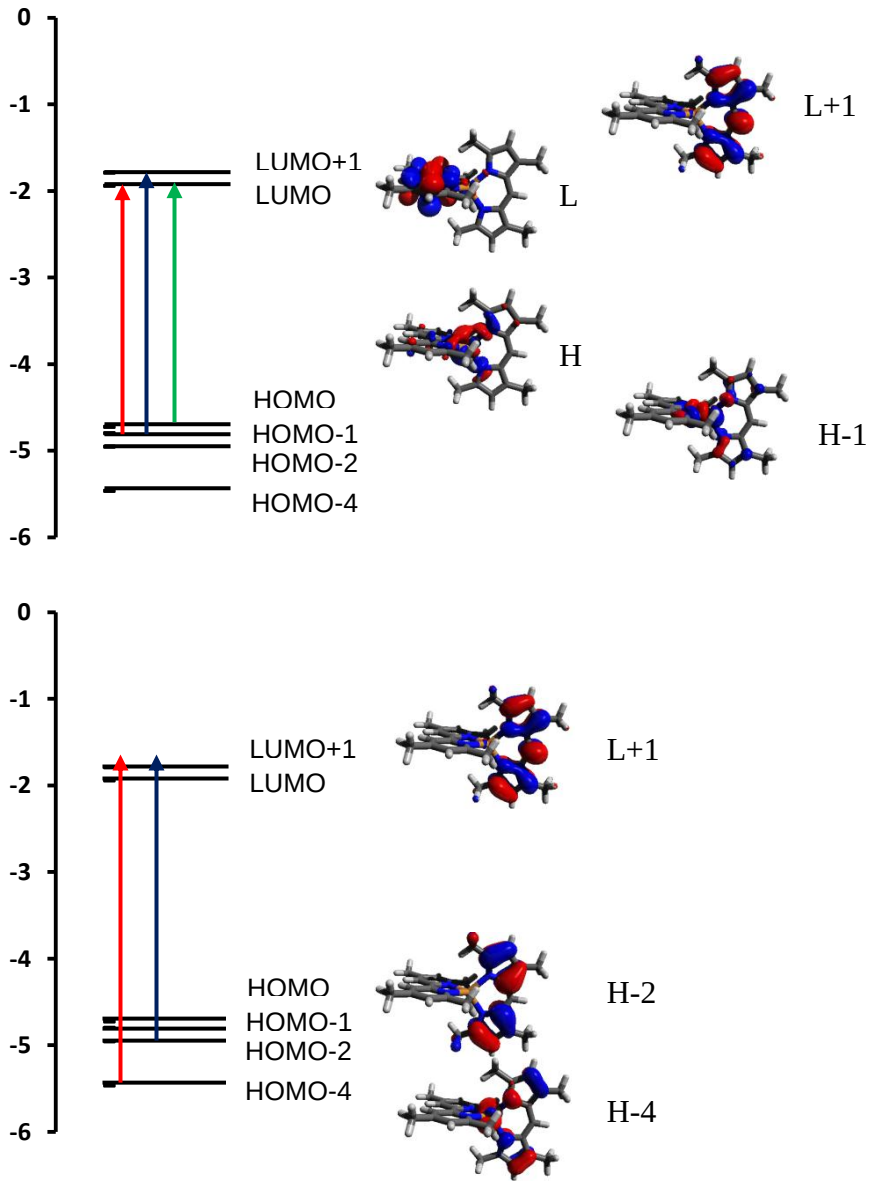

Figure S9 Molecular orbital diagrams for **1**, showing the main components of the transition for the calculated absorption at 581 nm (top) and 399 nm (bottom).

Supplementary Material (ESI) for Dalton Transactions
This journal is © The Royal Society of Chemistry 2013

Complex	MO	MO energy / eV	% Contribution from		
			Cu-based orbitals	Dipyrrin-based orbitals	Me-Bpy based orbitals
2	HOMO-10	-6.98	0.08	98.28	1.64
	HOMO-6	-6.50	2.08	96.40	1.52
	HOMO-4	-5.80	77.13	19.69	3.18
	HOMO-2	-5.19	72.11	14.63	13.26
	HOMO-1	-4.89	66.34	16.76	16.90
	HOMO	-4.73	0.16	99.64	0.20
	LUMO	-2.24	2.30	96.00	1.70
	LUMO+1	-1.95	2.49	3.41	94.10
	LUMO+2	-1.09	1.34	6.14	92.52
	LUMO+3	-0.93	0.59	97.13	2.28
	LUMO+4	-0.81	0.73	4.33	94.94
	LUMO+7	-0.40	0.64	97.18	2.18
	LUMO+9	-0.34	6.10	88.92	4.98

Table S3 Percentage contributions from component parts of **2** to selected molecular orbitals, and the calculated energies for these molecular orbitals.

Complex	Main Visible Absorbance / nm	Main Charge Transitions MO from	MO to	Relative Contribution
2	671	HOMO-2	LUMO	24 %
		HOMO-1	LUMO	62 %
		HOMO-1	LUMO+1	14 %
	541	HOMO	LUMO	66 %
		HOMO	LUMO+1	34 %
	375	HOMO-6	LUMO	12 %
		HOMO-2	LUMO+2	16 %
		HOMO	LUMO+3	72 %
	291	HOMO-10	LUMO	39 %
		HOMO-4	LUMO+3	11 %
		HOMO-4	LUMO+4	11 %
		HOMO-2	LUMO+7	13 %
		HOMO-2	LUMO+9	26 %

Table S4 TD-DFT calculated visible absorption wavelengths for **2**, indicating the molecular orbitals involved and their relative contribution to the absorption.

Supplementary Material (ESI) for Dalton Transactions
This journal is © The Royal Society of Chemistry 2013

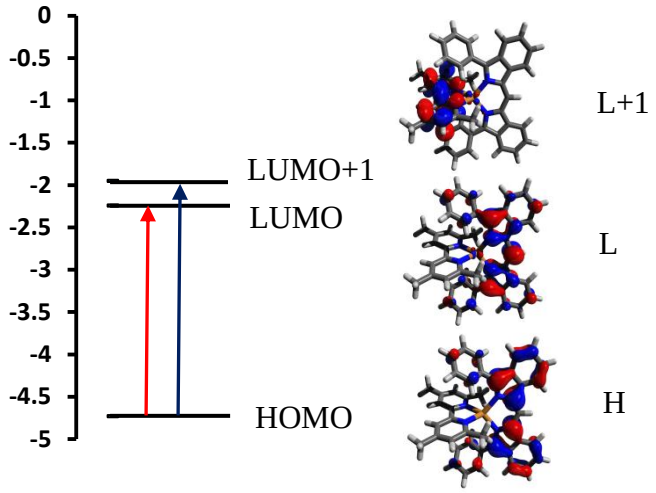

Figure S10 Molecular orbital diagram for **2**, showing the main charge transitions for the calculated absorption at 541 nm.

Complex	MO	MO energy / eV	% Contribution from		
			Cu-based orbitals	Dipyrrin-based orbitals	CO_2Et-Bpy based orbitals
3	HOMO-13	-7.16	1.73	33.39	64.88
	HOMO-9	-7.02	0.14	98.84	1.02
	HOMO-8	-6.85	34.17	58.75	7.08
	HOMO-7	-6.78	6.86	89.82	3.32
	HOMO-6	-6.56	2.43	96.19	1.38
	HOMO-3	-5.98	76.61	13.95	9.44
	HOMO-2	-5.56	69.26	16.82	13.92
	HOMO-1	-5.19	63.58	19.17	17.25
	HOMO	-4.78	0.12	99.70	0.18
	LUMO	-2.74	4.99	5.73	89.28
	LUMO+1	-2.31	2.06	95.82	2.12
	LUMO+2	-2.29	0.53	3.60	95.87
	LUMO+4	-0.97	0.67	98.75	0.58
	LUMO+5	-0.63	1.79	96.63	1.58
	LUMO+6	-0.46	0.32	97.56	2.12
	LUMO+9	-0.40	3.68	92.26	4.06

Table S5 Percentage contributions from component parts of **3** to selected molecular orbitals, and the calculated energies for these molecular orbitals.

Complex	Main Visible Absorbance / nm	Main Charge Transitions MO from	MO to	Relative Contribution
3	744	HOMO-2	LUMO	42 %
		HOMO-1	LUMO	58 %
	546	HOMO-3	LUMO	13 %
		HOMO-1	LUMO+2	60 %
		HOMO	LUMO+1	27 %
	538	HOMO-3	LUMO	28 %
		HOMO-1	LUMO+2	18 %
		HOMO	LUMO+1	54 %
	318	HOMO-13	LUMO	27 %
		HOMO-8	LUMO+1	24 %
		HOMO-6	LUMO+2	8 %
		HOMO-2	LUMO+4	20 %
		HOMO	LUMO+9	21 %
	316	HOMO-9	LUMO+1	9 %
		HOMO-7	LUMO+1	32 %
		HOMO-6	LUMO+1	30 %
		HOMO-1	LUMO+5	13 %
		HOMO	LUMO+4	9 %
		HOMO	LUMO+6	7 %

Table S6 TD-DFT calculated visible absorption wavelengths for **3**, indicating the molecular orbitals involved and their relative contribution to the absorption.

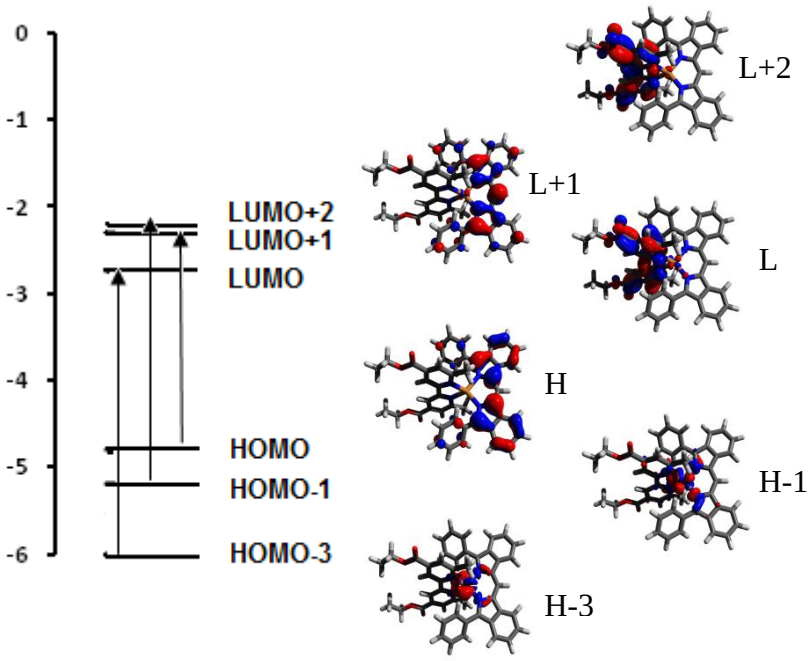

Figure S11 Molecular orbital diagram for **3**, showing the main charge transitions for the calculated absorption at 546 nm.

Solar Studies

Sample	Bipy used	Copper source	Solvent	Reducing agent or base
1	Dmdcbpy	$[Cu(CH_3CN)_4][BF_4]$	DCM	-
2	Dmdcbpy	$[Cu(CH_3CN)_4][BF_4]$	MeCN	-
3	Tcbpy	$[Cu(CH_3CN)_4][BF_4]$	MeCN	-
4	Dmdcbpy	$Cu(L1)_2$	MeOH	Methanol
5	Dmdcbpy	$Cu(L1)_2$	MeOH	Zn/Hg
6	Dmdcbpy	$Cu(L1)_2$	DCM	$NaBH_4$
7	Dmdcbpy	$[Cu(CH_3CN)_4][BF_4]$	DCM	NaOH
8	Dmdcbpy	$[Cu(CH_3CN)_4][BF_4]$	DCM	-
9	Dmdcbpy	$[Cu(CH_3CN)_4][BF_4]$	MeCN	-
10	Dmdcbpy	$Cu(L2)_2$	MeOH	-
11	Dmdcbpy	$[Cu(CH_3CN)_4][BF_4]$	MeCN	-

Table S7 Reagents and solvents used in each test. Bipy is adsorbed first followed by Cu and dipyrrin.

Sample	V_{oc} / mV	J_{sc} / $mAcm^{-2}$	V_{MP} / mV	J_{MP} / $mAcm^{-2}$	FF	η / %	Average η / %
REF	530	2.33	400	2.06	0.68	0.83	0.80 ± 0.03
1	520	0.40	420	0.30	0.62	0.13	0.10 ± 0.03
2	410	0.50	300	0.36	0.52	0.11	0.10 ± 0.01
3	410	0.26	300	0.19	0.56	0.06	0.05 ± 0.01
4	210	0.12	120	0.08	0.36	0.009	0.007 ± 0.02
8	280	0.03	170	0.02	0.39	0.003	0.002 ± 0.001
9	510	0.91	400	0.77	0.68	0.31	0.28 ± 0.03
10	420	0.46	320	0.35	0.56	0.11	0.09 ± 0.02
11	520	1.21	420	0.98	0.64	0.41	0.39 ± 0.02

Table S8 JV data collected at AM1.5. The unmasked area was 0.16 cm^2. Two cells per sample were tested and the average efficiency was recorded. The reported efficiency is the data of the best cell.

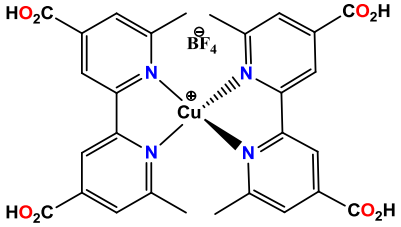

$Cu(dmdcbpy)_2BF_4$ (REF)

Supplementary Material (ESI) for Dalton Transactions
This journal is © The Royal Society of Chemistry 2013

Cyclic Voltammetry

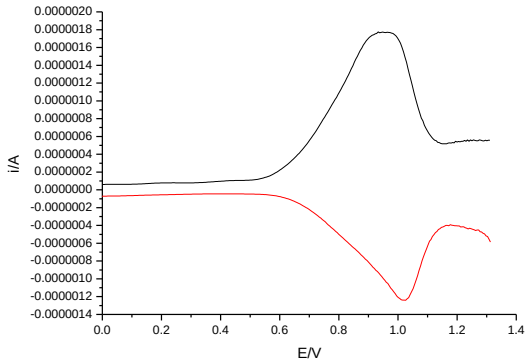

(a)

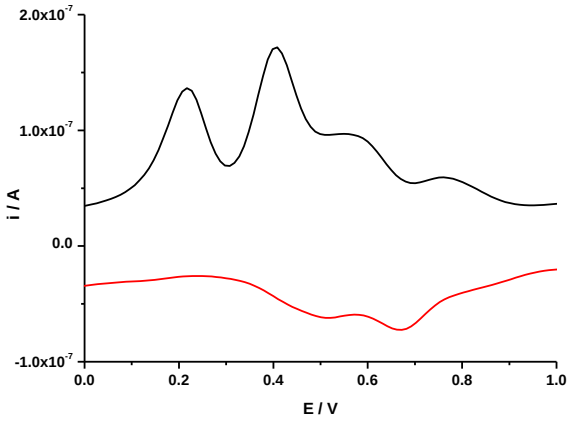

(b)

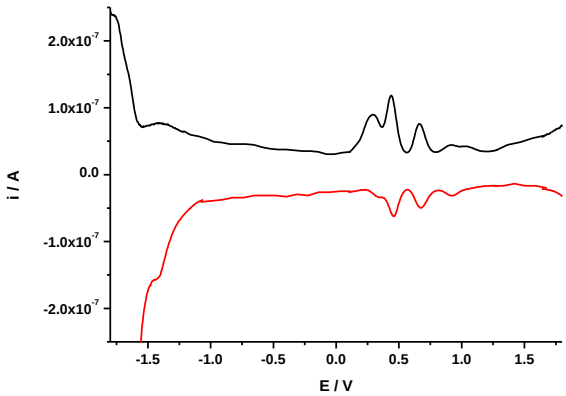

(c)

Supplementary Material (ESI) for Dalton Transactions
This journal is © The Royal Society of Chemistry 2013

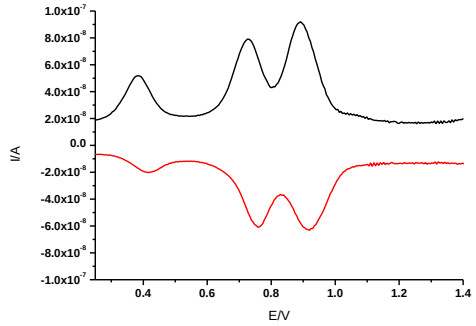

(d)

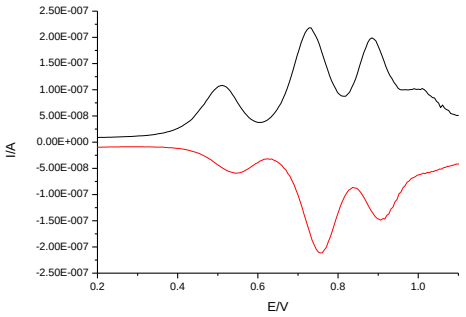

(e)

Figure S12 Oxidative differential pulse voltammetry of Cu(I) complexes against Ag/AgCl. Upper black scan is forward to more positive potential and the lower red line is the return scan. (a) **1** (b) **2** (c) **3** (d) **4** (e) **5**